

Realization of a classical counterpart of a scalable design for adiabatic quantum computation.

V. Zakosarenko, N. Bondarenko, S. H. W. van der Ploeg, A. Izmalkov,
S. Linzen, J. Kunert, M. Grajcar,* E. Il'ichev,† and H.-G. Meyer
*Institute for Physical High Technology,
P.O. Box 100239, D-07702 Jena, Germany*

(Dated: April 2, 2018)

We implement a classical counterpart of a scalable design for adiabatic quantum computation. The key element of this design is a coupler providing controllable coupling between two bistable elements (in our case superconducting rings with a single Josephson junction playing the role of a classical counterpart of superconducting flux qubits). The coupler is also a superconducting ring with a single Josephson junction that operates in the nonhysteretic mode with a screening parameter of about 0.9. The flux-coupling between two bistable rings can be controlled by changing the magnetic flux through the coupler. Since the coupling amplitude is proportional to the derivative of the coupler's current-flux relation, the coupling can be tuned from ferromagnetic to anti-ferromagnetic. In between the coupling can also be switched off.

PACS numbers: 85.25.Dq

The magnetic properties of a single-junction interferometer (superconducting loop with one Josephson junction) depend on its normalized critical current $\beta = 2\pi LI_C/\Phi_0$ only. Here L is the loop inductance, I_C the critical current of the junction and Φ_0 is the flux quantum. If $\beta > 1$ such an interferometer exhibits a double degenerated energy state if an external flux equal to half a flux quantum is applied (degeneracy point)¹. Close to the degeneracy point, the single junction ring is a bistable element with two magnetic moments corresponding to the superconducting screening currents flowing clockwise and counterclockwise. These two states can be described in spin formalism by making use of Pauli matrices. In other words, a system of magnetically coupled interferometers is a realization of a two-dimensional Ising spin system. When the coupling between spins is randomly distributed the system represents a spin glass. The problem of finding the ground state of such a system is a non-polynomial one, i.e., the amount of calculation resources needed grows exponentially with the number of elements. Mathematically this task is equivalent to solving the so-called MAXCUT problem.²

Recently, the implementation of an adiabatic quantum algorithm³ by making use of superconducting flux qubits has been proposed.^{4,5} Schematically, the implementation is the same as for the 2D Ising model described above but instead of classical bits quantum bits (qubits) are used. It has been shown that such a quantum system could solve the problem discussed above in polynomial time. In this letter we present the realization of a scalable classical design implementing the 2D Ising model with a coupling which can be tuned from antiferromagnetic, through zero, to ferromagnetic.

Theoretically several schemes of tunable coupling were proposed^{6,7} and also some implemented.^{8,9} In the design presented here we use the approach proposed by Maassen van den Brink *et al.*¹⁰ Here a coupler, realized as a single-

junction interferometer with $\beta_{CO} = 2\pi L_{CO}I_C/\Phi_0 < 1$, provides tunable coupling between two bistable elements. The coupling amplitude J can be varied by changing the magnetic flux through the coupler. The value of J is proportional to the derivative of the coupler's current-flux relation $I_s(\Phi_e)$, which presents itself as a periodic function versus external magnetic flux Φ_e . Therefore both antiferromagnetic and ferromagnetic couplings can be realized *in situ*. The coupling between interferometers could also be switched off when $dI_s/d\Phi_e = 0$. We have experimentally demonstrated both mentioned types of coupling and have been able to switch the coupling off in between.

The scalable design is build up out of basic cells, each containing one bistable element directly coupled to a readout DC-SQUID (superconducting quantum interference device) and two equal couplers coupled by flux transformers to the bistable element. In the basic cell there are also flux bias lines for each coupler and one for both the DC-SQUID and the bistable element. For the demonstration of the basic working principle we used a structure containing two basic cells of this scalable classical design. The samples were fabricated using our standard technology with Nb-AlO_x-Nb junctions.¹¹ The circuit diagram and a photograph of this investigated structure are shown in Fig.1.

The bistable elements (denoted by q, l and q, r , see Fig.1) are designed as interferometers with $\beta_q \sim 2.2$. The coupler is also designed as an interferometer with $\beta_{CO} \sim 0.9$. Two bistable elements, are coupled via a coupler and two flux transformers. The latter are used in order to increase the coupling between q, l and q, r and separate them in space. This resulted in reduction of unwanted crosstalk between the flux bias lines. Each bistable element shares a part of its inductance with the DC-SQUID used for its readout. The value of this inductance is optimized in such a way that the biasing of

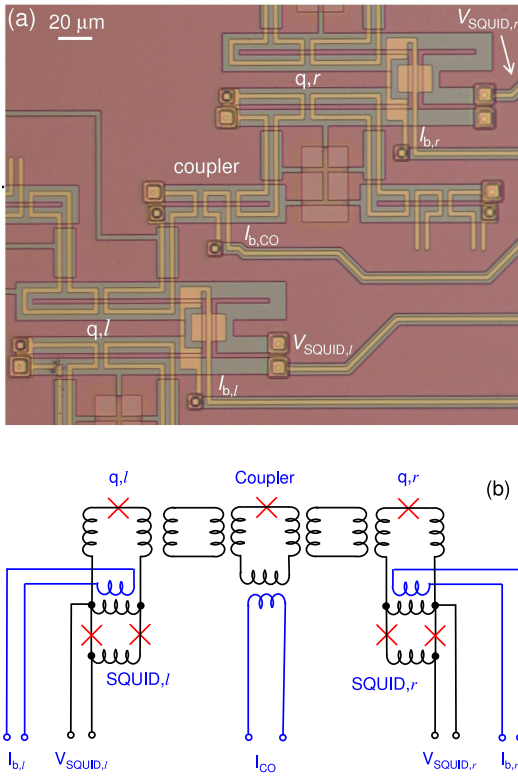


FIG. 1: (a) Photograph of the sample. (b) Circuit diagram. Two bistable elements (q,l and q,r) are coupled to each other by the coupler. The signals from bistable elements are read out by *left* and *right* SQUIDS. The fluxes through the interferometers could be controlled by the currents ($I_{b,l}$, $I_{b,r}$, I_{CO}) through the appropriate bias lines (b,l ; b,r ; and b,CO). All junctions are nominally the same: $3.5 \times 3.5 \mu\text{m}^2$.

the DC-SQUID does not change the state of the bistable element. A flux bias line coupled to this shared inductance can be used for the adjustment of the external flux through the DC-SQUID and interferometer as well as for feedback in a flux-locked-loop regime. All Josephson junctions are nominally the same ($3.5 \times 3.5 \mu\text{m}^2$). The desired screening factors for each element are achieved only by the loop's geometry. The effective inductances of the bistable elements, couplers, and DC-SQUIDS are designed taking into account the screening due to the coupling with closed superconducting loops. Their design values correspond to: $L_q = 60 \text{ pH}$, $L_{CO} = 25 \text{ pH}$, $L_{\text{SQUID}} = 50 \text{ pH}$.

The mutual inductances between bistable elements, DC-SQUIDS, couplers and appropriate bias lines were obtained from the measurements of switching current histograms as a function of the current through these lines. The mutual inductances found from these measurements are: $M_{b,l;\text{SQUID},l} \approx M_{b,r;\text{SQUID},r} = 5.4 \text{ pH}$, $M_{b,l;q,l} \approx M_{b,r;q,r} = 16 \text{ pH}$ and $M_{b,CO;\text{Coupler}} = 6.4 \text{ pH}$.

For the characterization of the coupler we measured the current induced in the right bistable element as a function of the current circulating in the left one, *i.e.* the response of the right DC-SQUID to the left bias-line

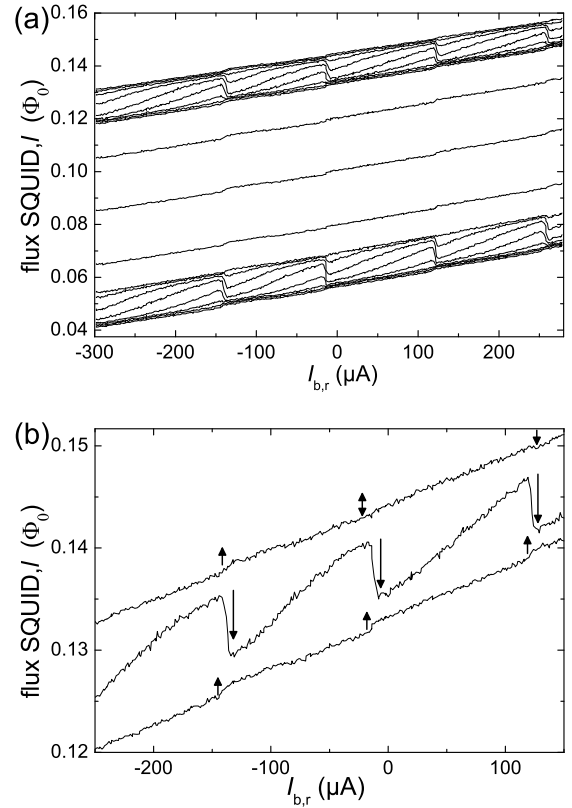


FIG. 2: Demonstration of tunable coupling between two bistable elements. (a) The output signal of the left DC-SQUID versus the current $I_{b,r}$ applied to the right bias line. The curves correspond to fixed bias current $I_{b,CO} = 524, 526, 528, 530, 532, 534, 536, 538$ and $540; 600, 700$ and $800; 850, 852, 854, 856, 858, 860, 862$ and $864 \mu\text{A}$ (from top to bottom) producing dominant magnetic flux in the coupler. The readout DC-SQUID operates in flux-locked-loop mode. (b) Curves from the upper panel for coupler's bias line current $I_{b,CO} = 526, 532$ and $540 \mu\text{A}$ (from top to bottom), the first curve is close to the transition from antiferromagnetic to ferromagnetic coupling. Since the magnetic flux through the coupler weakly depends also on $I_{b,r}$, the gradual crossover from antiferromagnetic to ferromagnetic regime is driven by the right bias line current. The up, up-down, and down arrows denote antiferromagnetic, “zero”, and ferromagnetic couplings, respectively.

current (see Fig.1) and *vice versa*. For the measurements the DC-SQUID was shunted with an external resistor soldered onto the sample holder. The DC-SQUID was operated in flux-locked-loop mode making use of standard room temperature electronics¹². The electronics amplifies the DC-SQUID voltage and supplies the feedback current through the appropriate bias line, keeping the total flux in the DC-SQUID constant. For our design it means that the output signal of the DC-SQUID electronics is proportional to the screening current in the interferometer which is roughly proportional to the flux coupled to it because $\beta_q > 1$. The measurements were carried out in liquid He at 4.2 K.

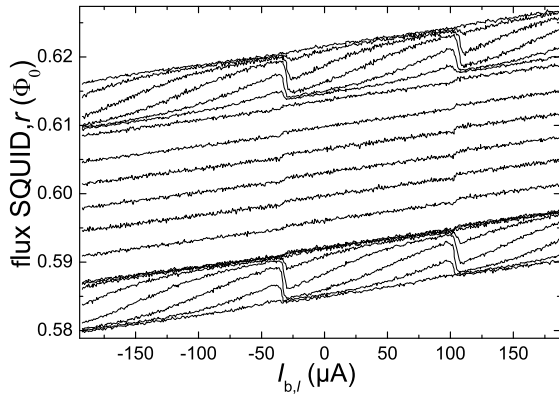


FIG. 3: Output signal of the right DC-SQUID versus the current $I_{b,l}$ applied to the left bias line. The current trough the coupler are from top to bottom $I_{b,CO} = 530, 528, 526, 524, 522, 520$ and $518; 510, 460, 410, 360$ and $310; 210, 208, 206, 204, 202, 200, 198$ and $196 \mu\text{A}$.

The coupling strength J between the interferometers q,l and q,r was tuned by applying a magnetic flux Φ_e through the coupler using its bias line $\propto I_{b,CO}$ (see Fig.1). The value of J increases with the coupler's screening factor β_{CO} . On the other hand, $\beta_{CO} < 1$ is required in order to obtain the change of the coupling sign. Thus, for optimal results we need a sample with $\beta_{CO} \lesssim 1$. Taking into account the coupler inductance $L_{CO} = 25 \text{ pH}$, we fabricated samples with the junction oxidation process for $j_c = 100 \text{ A/cm}^2$ giving a critical current for the junction $I_C \approx 12 \mu\text{A}$ and $\beta_{CO} \approx 0.9$ close to unity.

The results are shown in Fig.2 were the left DC-SQUID is used as a measuring device and in Fig.3 for measurements with the right DC-SQUID. The slope of the curves is due to the direct parasitic coupling between the right (left) bias line and the left (right) bistable element. The periodical modulation of these curves is due to the jumps of screening current of the right (left) interferometer. Note that the period of this modulation is the same as the period measured with the DC-SQUIDS directly cou-

pled to the interferometer confirming that we are looking at the effect of this interferometer.

In Figs.2 and 3 the curves with upward and downward kinks correspond to antiferromagnetic and ferromagnetic couplings, respectively. The rounding is due to an averaging of the thermally activated jumps between two stable branches of the interferometer. The kink height is proportional to the derivative of the couplers' current phase relation: $dI/d\Phi_e = 2\pi I_C \cos \phi / [\Phi_0(1 + \beta_{CO} \cos \phi)]$ with $\phi = 2\pi\Phi_e/\Phi_0 - \beta_{CO} \sin \phi$ the phasedrop over the coupler junction. So the maximal kink heights in the ferro- and antiferromagnetic cases are proportional to $\beta_{CO}/(1 - \beta_{CO})$ and $\beta_{CO}/(1 + \beta_{CO})$, respectively. The observed ratio of the maximal kink height for these two cases 12:1 corresponds to $\beta_{CO} = 0.85$ which is in reasonable agreement with the expected value. Also, the fact that the ferromagnetic coupling region is smaller than the anti-ferromagnetic one qualitatively agrees with this picture. However, the experimentally observed width of this region is only $0.04 \Phi_0$ while this simple model would predict $0.23 \Phi_0$ for $\beta_{CO} = 0.85$. This could be due to a non-sinusoidal current phase relation of the coupler junction. Further experiments would be necessary to clear up this disagreement. In between the ferro- and the antiferromagnetic regions the coupling vanishes as indicated by the updown arrow.

In conclusion, we demonstrate tunable coupling between two single junction interferometers in classical mode. We show both ferromagnetic and antiferromagnetic type of coupling, including zero coupling between these two regimes. This system enables to study relaxation and annealing in spin glass.

S.v.d.P., A.I., E.I. were supported by the EU through the RSFqubit and EuroSQIP projects and M.G. by Grants VEGA 1/2011/05, APVT-51-016604 and the Alexander von Humboldt Foundation. We thank H. E. Hoenig for fruitful discussions. We also thank J. Hilton for comments.

Partial financial support by the D-Wave Systems Inc. is gratefully acknowledged.

* On leave from Department of Experimental Physics, Comenius University, SK-84248 Bratislava, Slovakia.

† Electronic address: ilichev@ipht-jena.de

¹ A. Barone and G. Paterno, *Physics and Applications of the Josephson Effect* (John Wiley & Sons, New York, 1982).

² M. R. Garey, D. S. Johnson, and L. Stockmeyer, *Theor. Comput. Sci.* **1**, 237 (1976).

³ E. Farhi, J. Goldstone, S. Gutmann, J. Laplan, A. Lundgren, and D. Preda, *Science* **292**, 472 (2001).

⁴ W. M. Kaminsky, Seth Lloyd, and T. P. Orlando, *quant-ph/0403090*.

⁵ M. Grajcar, A. Izmalkov, and E. Il'ichev, *Phys. Rev. B* **71**, 144501 (2005).

⁶ J. Clark, T.L. Robertson, B.L.T. Plourde, A. García-Martínez, P.A. Reichardt, D.J. van Harlingen, B. Chesca, R. Kleiner, Y. Makhlin, G. Schön, A. Shnirman and F.K.

Wilhelm, *Phys. Scr.*, **T 102**, 173 (2002).

⁷ T. V. Filippov, S.K. Tolpygo, J. Mannik, and J.E. Lukens, *IEEE Trans. Appl. Supercond.* **13**, 1005 (2003).

⁸ M. G. Castellano, F. Chiarello, R. Leoni, D. Simeone, G. Torrioli, C. Cosmelli and P. Carelli, *Appl. Phys. Lett.* **86**, 152504 (2005).

⁹ S.H.W. van der Ploeg, A. Izmalkov, Alec Maassen van den Brink, U. Hübner, M. Grajcar, E. Il'ichev, H.-G. Meyer and A.M. Zagoskin, *Phys. Rev. Lett.* **98**, 057004 (2007).

¹⁰ A. Maassen van den Brink, A.J. Berkley, M. Yalowsky, *New Journal of Physics* **7**, 230 (2005).

¹¹ R. Stolz, L. Fritzsche, and H.-G. Meyer, *Supercond. Sci. Technol.* **12**, 806–808 (2005).

¹² www.supracon.com